flight path along with most efficient use of thrust to accelerate the rocket to orbital speed at the lowest possible altitude. In the case of the shuttle, the thrust angle has to be positive (but generally decreasing) during final acceleration to orbital speed (which results in the larger steering losses). The Hohmann type of ascent is slightly more efficient than the shuttle type of ascent (in getting the greatest weight into orbit), but it takes nearly twice as long. In turn, the shuttle type of ascent takes considerably longer than direct ascent. The primary advantage of Hohmann ascent or shuttle ascent over direct ascent is that the same weight rocket can deliver about 16% more total weight to the 240-mile orbit of the International Space Station (ISS). For subsonic air launch (at about 40,000-ft altitude and high flight-path angle) of a miniature rocket weighing 7000 lb, the total weight delivered to the ISS orbit increases from about 128 lb to about 150 lb in changing from direct ascent to either shuttle or Hohmann ascent. It is conjectured that the disparity in total weight placed in orbit should increase with an increase in orbital altitude.

References

[1]Wall, R., "New Launcher Eyed for Small Satellites," *Aviation Week and Space Technology*, Vol. 155, No. 19, 2001, pp. 64, 65.

[2]Isakowitz, S. J., Hopkins, J. P., Jr., and Hopkins, J. B., *International Reference Guide to Space Launch Systems*, 3rd ed., AIAA, Reston, VA, 1999, pp. 267–279.

[3]Boltz, F. W., "Low-Cost Small-Satellite Delivery System," *Journal of Spacecraft and Rockets*, Vol. 39, No. 5, 2002, pp. 818–820.

[4]Humble, R. W., Henry, G. N., and Larson, W. J. (eds.), *Space Propulsion Analysis and Design*, McGraw–Hill, New York, 1995, pp. 47–52.

[5]Boltz, F. W., "Analytic Solution for Vertical Launch into Orbit," *Journal of the Astronautical Sciences*, Vol. 37, No. 4, 1989, pp. 491–511.

[6]Logsdon, T., *Orbital Mechanics, Theory and Application*, Wiley, New York, 1998, p. 155.

J. Martin
Associate Editor

Oblate Earth Eclipse State Algorithm for Low-Earth-Orbiting Satellites

Sima Adhya,* Anthony Sibthorpe,† Marek Ziebart,‡ and Paul Cross§
University College London, London, England WC1E 6BT, United Kingdom

Introduction

EARTH-ORBITING satellites experience partial or total eclipses when they pass through the regions known as the umbra and penumbra. In the penumbra, the total solar irradiance is partially occluded by the Earth, whereas the umbra can be defined as the region on the antisun side of the Earth, which is completely devoid of solar radiation.

Figure 1 shows the umbra and penumbra regions for a spherical Earth. In reality, the Earth is flattened, with the polar radius being about 0.3% smaller than the equatorial radius. If the Earth's oblateness is taken into account, the boundaries of the shadow regions are altered.

Received 23 April 2003; revision received 24 July 2003; accepted for publication 11 September 2003.

*Research Student, Department of Geomatic Engineering; sima@ge.ucl.ac.uk. Member AIAA.

†Research Student, Department of Geomatic Engineering; ants@ge.ucl.ac.uk.

‡Lecturer, Department of Geomatic Engineering.

§Leica Professor of Geomatic Engineering, Department of Geomatic Engineering.

To model accurately the forces acting on the satellite due to solar radiation, it is important to know exactly when the satellite enters or exits a shadow region because the amount of solar radiation incident on the spacecraft drops dramatically. Examples of forces so affected include solar radiation pressure and the recoil force induced by thermal reradiation.

It is perhaps surprising, then, that literature on this topic is so sparse and that the existing material ranges between two extremes. Several techniques use a spherical Earth model because this allows simple geometric arguments to be developed.[1–4] However, it is certainly worthwhile treating the Earth as an oblate spheroid because it has been shown that, with respect to a spherical Earth, the main changes occur in the timing of the umbra and penumbra transitions and in the overall duration of the eclipse periods.[5] Such mistiming has important consequences for the precise numerical integration of orbit trajectories.[6] The main drawback of implementing such a model is that existing approaches for eclipse boundary determination with a spheroidal Earth are significantly more complex than for a spherical Earth. As a result, existing models using a spheroidal Earth are costly to implement in operational software because they are computationally intensive, requiring the use of either a series of rotations[5] or the solution of a quartic equation.[3]

As part of the force modeling work undertaken at University College London by its Geodesy Research Group, a new treatment of the problem has been developed that yields direct solutions for the eclipse state while still accounting for the Earth's polar flattening. This Note presents the mathematical formulation of the method and initial results.

Method to Determine Satellite State

An instantaneous plane is defined by the geocenter, the Earth–sun vector $\boldsymbol{r}_s$ and the Earth–spacecraft vector $\boldsymbol{a}$. In this two-dimensional space, the sun is modeled as a circle. The unit vector orthogonal to the Earth–sun vector is used to find the two required edges of the sun in an Earth centered inertial (ECI) coordinate frame (Fig. 1). The vectors $\boldsymbol{r}_{s1}$ and $\boldsymbol{r}_{s2}$ can be defined as the lines from the geocenter to sun-edge 1 and sun-edge 2, respectively. The method is based on tests that determine whether or not lines from the sun edges to the spacecraft intersect the Earth. If an intersection occurs, and the distance from the sun to this intersection point is less than the sun–spacecraft distance, then the satellite is either in the penumbra or the umbra.

The actual calculations of the intersection points are carried out using three-dimensional geometry, with the surface of the Earth being mathematically approximated by the equation of a spheroid:

$$(x^2 + y^2)/p^2 + z^2/q^2 = 1 \tag{1}$$

where x, y, and z are the ECI coordinates of a point in space on the surface of the spheroid, p is the equatorial radius, and q is the polar radius.

The two lines between the spacecraft and the sun can be defined as follows:

$$(x - a_1)/b_1 = (y - a_2)/b_2 = (z - a_3)/b_3 \tag{2}$$

where a_1, a_2, and a_3 are the x, y, and z components of the position vector of the spacecraft $\boldsymbol{a}$, and b_1, b_2, and b_3 are the x, y, and z components of the vector from either sun-edge 1 or sun-edge 2 to the spacecraft, $\boldsymbol{b}$. Vectors $\boldsymbol{a}$ and $\boldsymbol{b}$ can be obtained for a specific epoch, and hence, the lines are defined. In the plane, rays of light starting at the sun edges and making tangents with the Earth define the full phase/penumbra and penumbra/umbra boundaries, as shown in Fig. 2.

To determine $\hat{\boldsymbol{s}}_p$, the cross product between $\boldsymbol{r}_s$ and $\boldsymbol{a}$ is taken to give a vector $\boldsymbol{r}_i$ normal to the plane:

$$\boldsymbol{r}_i = \boldsymbol{r}_s \times \boldsymbol{a} \tag{3}$$

Taking the cross product of $\boldsymbol{r}_i$ with $\boldsymbol{r}_s$ gives the vector that lies in the plane and is perpendicular to $\boldsymbol{r}_s$, which is $\boldsymbol{s}_p$:

$$\boldsymbol{s}_p = \boldsymbol{r}_s \times \boldsymbol{r}_i \tag{4}$$

Normalizing this vector gives $\hat{\boldsymbol{s}}_p$.

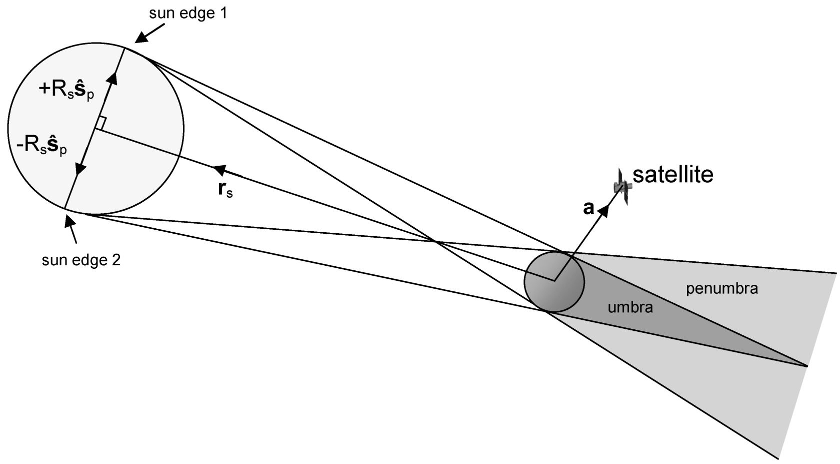

Fig. 1 Lines forming shadow region boundaries in a plane defined by the sun center, the geocenter, and the satellite.

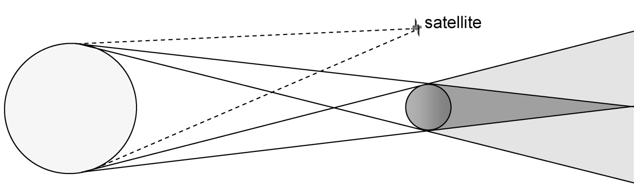

a) Full phase: no lines intersect

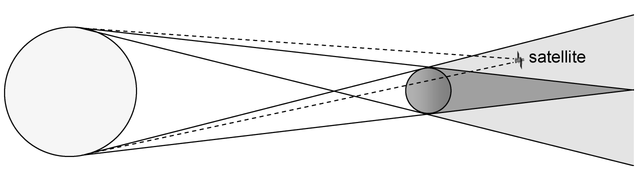

b) Penumbra: one line intersects

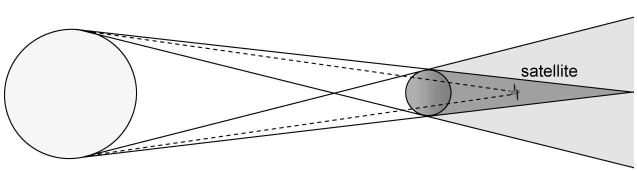

c) Umbra: both lines intersect Earth

Fig. 2 Satellite in full phase and satellite in eclipse.

The two sun-edge points are given by

$$\boldsymbol{r}_{s1} = \boldsymbol{r}_s + (R_s \hat{\boldsymbol{s}}_p) \tag{5}$$

$$\boldsymbol{r}_{s2} = \boldsymbol{r}_s - (R_s \hat{\boldsymbol{s}}_p) \tag{6}$$

where R_s is the sun radius.

The vector $\boldsymbol{b}$ is

$$\boldsymbol{b} = \boldsymbol{r}_{sc} - \boldsymbol{r}_{s1} \tag{7}$$

for line 1 and

$$\boldsymbol{b} = \boldsymbol{r}_{sc} - \boldsymbol{r}_{s2} \tag{8}$$

for line 2.

From Eq. (2), it is possible to rewrite y and z as a function of x and the coefficients of vectors $\boldsymbol{a}$ and $\boldsymbol{b}$:

$$y = (b_2/b_1)(x - a_1) + a_2 \tag{9}$$

$$z = (b_3/b_1)(x - a_1) + a_3 \tag{10}$$

Now y and z can be substituted into Eq. (1) to yield a quadratic in x:

$$\frac{x^2 + [(b_2/b_1)(x - a_1) + a_2]^2}{p^2} + \frac{[(b_3/b_1)(x - a_1) + a_3]^2}{q^2} = 1 \tag{11}$$

$$q^2x^2 + q^2\left[\frac{b_2}{b_1}(x - a_1) + a_2\right]^2 + p^2\left[\frac{b_3}{b_1}(x - a_1) + a_3\right]^2 = p^2q^2$$

$$Ax^2 + Bx + C = 0 \tag{12}$$

In this quadratic,

$$A = b_1^2q^2 + q^2b_2^2 + p^2b_3^2$$

$$B = -2b_2^2q^2a_1 + 2b_1q^2a_2 - 2p^2b_3^2a_1 + 2p^2b_1a_3$$

$$C = q^2\left[b_1^2a_2^2 - b_2^2a_1^2 - 2b_2b_1a_1a_2\right] + p^2\left[b_1^2a_3^2 - b_3^2a_1^2 - 2b_3b_1a_1a_3\right] - b_1^2p^2q^2 = 0 \tag{13}$$

The real solutions to this quadratic equation give the x coordinates of the points of intersection of the spheroid and the sun edge to spacecraft line.

For a real solution to exist,

$$B^2 - 4AC \geq 0 \tag{14}$$

If Eq. (14) is satisfied, an intersection takes place. A negative value has no physical meaning, but shows that no intersection occurs. If there is no intersection, then the satellite is in full phase. Lines from both sun edges to an instantaneous satellite position are tested in this manner. Once the value of x is obtained, it can be substituted into Eq. (2) to solve for the y and z coordinates of the intersection point; equivalent equations can be generated to yield quadratics in y and z. Full coordinates of the intersection point are required to calculate its distance from the sun. If this distance is larger than the distance between the sun and the spacecraft, then the satellite is automatically assigned a state of full phase. In all other cases, the following conditions are regarded:

1) If both lines have real solutions, then the spacecraft is in the umbra.

2) If only one of the lines has real solutions, the spacecraft is in the penumbra.

3) If there are no real solutions, then the spacecraft is in full phase.

The algorithm written to carry out this function takes a Universal Time Coordinated timetag and the position vector of the satellite as inputs. The corresponding sun positions are retrieved for each epoch from an ephemeris file (Jet Propulsion Laboratory, California Institute of Technology, JPL DE405), and the test for intersection points is carried out. A specified integer value is returned depending on the result of the computation; the program calling the function uses this integer value to determine if a change of state has occurred.

Results

The preceding method describes a way of determining whether the satellite is in full phase, penumbra, or umbra at a particular epoch. This algorithm can be used with positions interpolated from precise

Table 1 Eclipse entry/exit time offsets between different models and Envisat photometry

Date	Time from photometry	Spheroid, s	Sphere, s	IERS, s
17/02/2003	20:36:59	−4	2	12
17/02/2003	22:17:31	−0.5	6	15
18/02/2003	21:45:52	−4	−1	8
17/03/2003	20:53:54	2	8	17
18/03/2003	20:22:15	−2	4	12
18/03/2003	22:02:53	−5	1	10
20/03/2003	20:59:19	2	8	17
21/03/2003	22:08:14	0	6	14
23/03/2003	21:04:44	3	9	18
24/03/2003	20:33:02	2	8	16
27/03/2003	20:38:28	2	8	16
27/03/2003	22:19:04	1	7	16
07/04/2003	21:31:58	2	7	16
rms		2.649383	6.379052	14.67337

Table 2 Approximate orbital elements for Envisat

Parameter	Value
Semi-major axis, km	7159
Inclination, deg	98.5
Eccentricity	0.001165
Argument of perigee, deg ±3 deg	90.0
Mean local solar time at descending node	10 a.m.

ephemeredes (as used here), or from an integrated orbit position for prediction purposes. Precise orbit determination requires an accurate timetag for when a change of state occurs[6] because this is important when calculating the correct solar flux for use in modeling many nonconservative forces. To predict the exact crossing time, iteration between the satellite's position and its state will be required. The iteration process is efficient because the method shares much of the geometric simplicity of its spherical Earth counterparts, thus also making its implementation very straightforward. The algorithm could be easily incorporated into both fixed-step and adaptive-step size orbit integrators.

Preliminary analyses were conducted with precise Envisat orbit and photometric data provided by the satellite laser ranging facility at Herstmonceux. Table 1 shows the time offsets for a series of eclipse entry/exit times between photometric observations and three different Earth models. A small rms value for these time offsets suggests a greater degree of accuracy in the model. The spheroidal model uses the algorithm described here with $p = 6378.137$ km and $q = 6356.752$ km[1], the spherical model uses $p = q = 6378.137$ km and the International Earth Rotation Service (IERS) model uses a spherical Earth with $p = q = 6402.0$ km (Ref. 7). The data indicate that, with standard values for the Earth radii, the given spheroidal algorithm can determine shadow crossing times that demonstrate a significant improvement over comparable spherical models for a low-Earth-orbiting satellite when tested against photometric observations. For low-Earth-orbiting satellites, an incorrect transition point will introduce a systematic bias over many orbit revolutions. Polar orbiters, such as Envisat (Table 2), will be subject to a difference of up to 4 min spent in eclipse when those predicted by a spherical Earth model are compared against those from the current algorithm.

In terms of efficiency, the algorithm developed here runs 13.4 times faster than an alternative oblate Earth technique[5] when 1 million eclipse states are determined on a dual processor AMD Athlon 2200+ machine.

Conclusions

The main operational software requirements for the computation of precise orbit trajectories are accuracy and efficiency. An important part of this must be the correct determination of eclipse shadow boundary-transition times. A review of the publicly available literature on this subject has convinced the present authors that current methods are either accurate or efficient, but not both. By modeling the Earth as a spheroid, this method retains the physical complexity inherent in the problem. Yet the algorithm is as simple computationally as techniques that model the Earth as a sphere, making our approach highly efficient. Indeed, initial results point to the ability of our algorithm to be able to determine shadow crossing times to within 1 s for low-Earth-orbiting satellites when compared to photometric observations (Envisat and ERS-2).

Acknowledgments

This work was funded by the Engineering and Physical Sciences Research Council and the Natural Environment Research Council under its Earth Observation Centre of Excellence program. The authors thank the staff of the satellite laser ranging facility at Herstmonceux, East Sussex, for supplying the photometric data that were used for initial validation.

References

[1]Montenbruck, O., and Gill, E., *Satellite Orbits: Models, Methods and Applications*, Springer-Verlag, Berlin, 2000, pp. 80–83.

[2]Vallado, D., *Fundamentals of Astrodynamics and Applications*, 2nd ed., Microcosm Press and Kluwer Academic, Norwell, MA, 2001, pp. 285–291.

[3]Neta, B., and Vallado, D., "On Satellite Umbra/Penumbra Entry and Exit Positions," *Advances in the Astronautical Sciences 95(II): Spaceflight Mechanics 1997*, edited by K. C. Howell, D. A. Ciddi, J. E. Cochran, and T. S. Kelso, Univelt, San Diego, CA, 1997, pp. 715–724.

[4]Vokrouhlický, D., Farinella, P., and Mignard, F., "Solar Radiation Pressure Perturbations for Earth Satellites I. A Complete Theory Including Penumbra Transitions," *Astronomy and Astrophysics*, Vol. 280, Dec. 1993, pp. 295–312.

[5]Vokrouhlický, D., Farinella, P., and Mignard, F., "Solar Radiation Pressure Perturbations for Earth Satellites IV. Effects of the Earth's Polar Flattening on the Shadow Structure and the Penumbra Transitions," *Astronomy and Astrophysics*, Vol. 307, March 1996, pp. 635–644.

[6]Woodburn, J., "Effects of Eclipse Boundary Crossings on the Numerical Integration of Orbit Trajectories," AIAA Paper 2000-4027, Aug. 2000; also URL: http://www.stk.com/pdf/white_papers/0800_shadow_boundary.pdf [cited 22 February 2003].

[7]McCarthy, D., International Earth Rotation Service, IERS TN 21, IERS Conventions, Observatoire de Paris, Paris, 1996, p. 81.

C. Kluever
Associate Editor